Supplement of The Cryosphere, 10, 1721–1737, 2016
http://www.the-cryosphere.net/10/1721/2016/
doi:10.5194/tc-10-1721-2016-supplement

The Cryosphere Open Access

Supplement of

Evaluation of air–soil temperature relationships simulated by land surface models during winter across the permafrost region

Wenli Wang et al.

Correspondence to: Duoying Ji (duoyingji@bnu.edu.cn)

Supplementary Tables

SI Table 1. Climate data sets used to drive each model.

Model	Climate forcing data
CLM4.5	CRUNCEP4[1]
CoLM	Princeton[2]
ISBA	WATCH (1901-2010)[3]
JULES	WATCH (1901-2001)[3]
LPJ-GUESS	CRU TS 3.1[4]
MIROC-ESM	CMIP5 Drivers[5], WATCH (1901-1978)[3]
ORCHIDEE	WFDEI (1978-2009)[6]
UVic	CRUNCEP4[1], CRU[7], UDel[8]
UW-VIC	NCEP-NCAR[9]

[1]Viovy and Ciais (2011) (http://dods.extra.cea.fr/)

[2]Sheffield et al. (2006) (http://hydrology.princeton.edu/data.pgf.php)

[3]Weedon et al. (2011) (http://www.waterandclimatechange.eu/about/watch-forcing-data-20th-century)

[4]Harris et al. (2013), University of East Anglia Climate Research Unit

[5]Watanabe et al. (2011)

[6]http://www.eu-watch.org/gfx_content/documents/README-WFDEI.pdf

[7]Mitchell and Jones (2005) for temperature

[8]Willmott and Matsura (2001) for precipitation

[9]Kalnay et al. (2006)

Harris, I., Jones, P.D., Osborn, T.J., and Lister, D.H.: Updated high-resolution grids of monthly climatic observations. Int. J. Clim., doi: 10.1002/joc.3711, 2013.

Kalnay, E. et al.: The NCEP Climate Forecast System. J. Clim., 19, 3483.3517 , 2006.

Mitchell, T.D., and Jones, P.D.: An improved method of constructing a database of monthly climate observations and associated high-resolution grids, Int. J. Clim., 25(6), 693-712, doi: 10.1002/joc.1181, 2005.

Sheffield, J., Goteti, G., and Wood, E.F.: Development of a 50-yr high-resolution global dataset of meteorological forcings for land surface modeling, J. Clim., 19, 3088-3111, 2006.

Viovy, N. and Ciais, P.: CRUNCEP data set for 1901–2008, Tech. Rep. Version 4, Laboratoire des Sciences du Climat et de l'Environnement, 4078, 4122, 2011.

Watanabe, S. et al.: MIROC-ESM 2010: model description and basic results of CMIP5-20c3m experiments. Geosci. Model Dev., 4, 845–872, doi:10.5194/gmd-4-845-2011, 2011.

Weedon, G.P., Gomes, S., Viterbo, P., Shuttleworth, W.J., Blyth, E., Österle, H., Adam, J.C., Bellouin, N., Boucher, O., and Best, M.: Creation of the WATCH Forcing data and its use to assess global and regional reference crop evaporation over land during the twentieth century. J. Hydromet., 12, 823-848, doi: 10.1175/2011JHM1369.1, 2011.

Willmott, C.J., and Matsuura, K.: Terrestrial air temperature and precipitation: monthly and annual time series (1950-1999) (version 1.02), Center for Climate Research, University of Delaware, Newark, DE, 2001.

SI Table 2. Russian-station-location averaged error statistics for air temperature (℃) and precipitation (mm/d) for winter 1980-2000. For each variable, the maximum available number of observations (n) is used. $mean_{obs}$ and $stdev_{obs}$ are the station-observed mean and interannual variability (standard deviation), while stdev is the standard deviations of each model. Both, air temperature and precipitation are from the climate forcing data sets for all models, except for MIROC-ESM which simulates both. BIAS is the mean error 'model minus observation', RMSE is the root-mean-square error, and both represent biases in the climate forcing compared to the station observations (except for MIROC-ESM).

	Air temperature (n=518) $mean_{obs}$= -16.3 ℃ $stdev_{obs}$=2.2 ℃			Precipitation (n=512) $mean_{obs}$=0.89 mm/d $stdev_{obs}$=0.5 mm/d		
	BIAS	RMSE	stdev	BIAS	RMSE	stdev
CLM4.5	-4.7	5.0	2.0	-0.05	0.6	0.1
CoLM	-0.9	2.0	2.1	0.3	0.7	0.3
ISBA	-1.6	2.3	2.2	0.2	0.6	0.3
JULES	-2.5	2.9	2.3	0.2	0.6	0.3
LPJ-GUESS	-0.8	2.0	2.1	-0.03	0.5	0.1
MIROC-ESM	2.7	5.2	2.2	0.5	0.9	0.3
ORCHIDEE	-1.4	2.4	2.2	0.3	0.6	0.3
UVic	-1.8	2.5	2.1	-0.2	0.6	0.1
UW-VIC	-1.1	2.2	2.1	0.3	0.6	0.4

Supplementary Figures

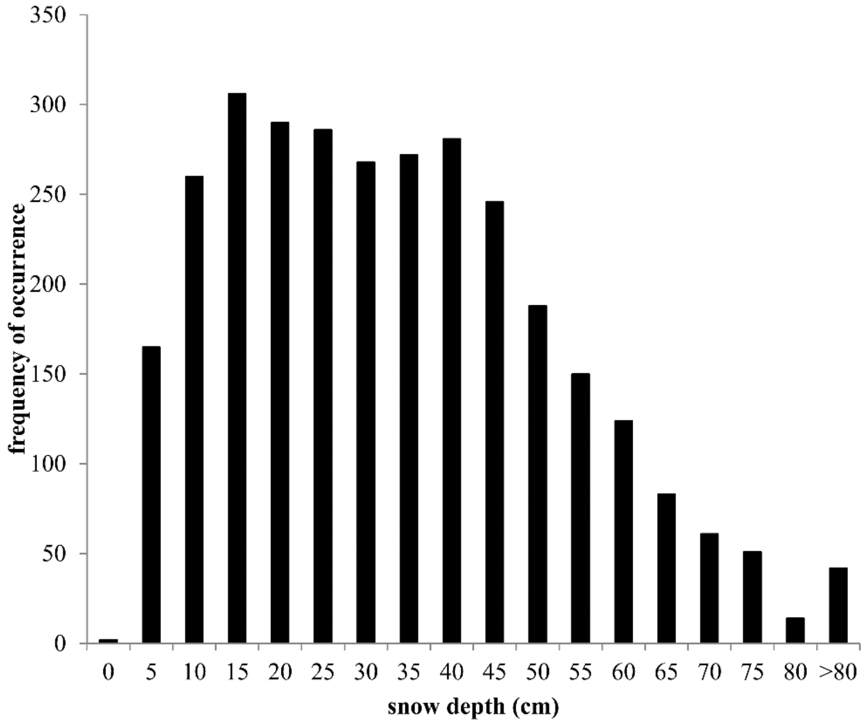

SI Figure 1. Histogram of seasonal winter mean snow depth from 268 Russian stations between 1980-2000.

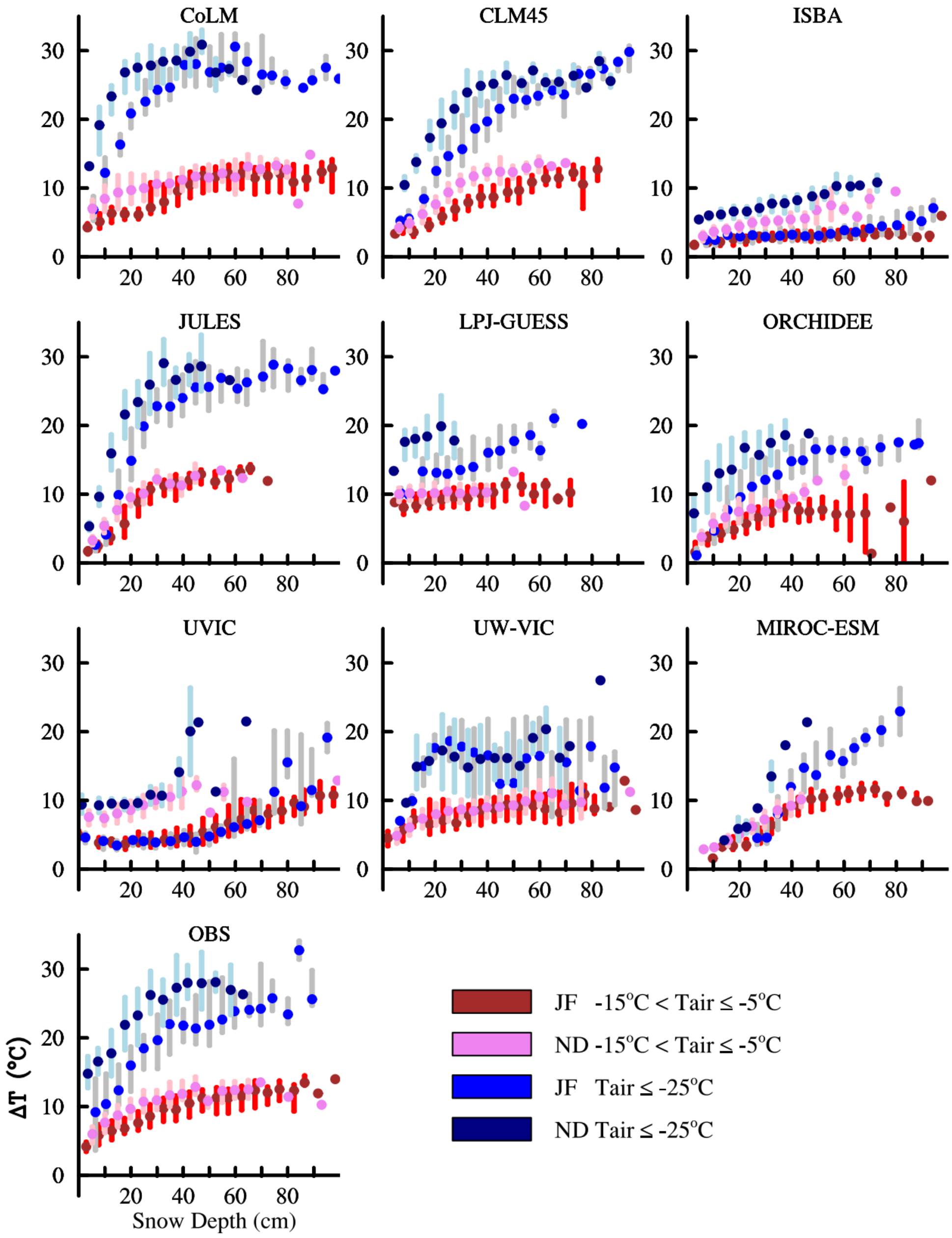

SI Figure 2. Variation of ΔT (℃) (the difference between soil temperature at 20 cm depth and air temperature) with snow depth (cm) for winter 1980-2000. The dots represent the medians of 5 cm snow depth bins and the upper and lower bars indicate the 25th and 75th percentiles, calculated from all Russian station grid points (n=268) and 21 individual winters. Color represents two different air temperature regimes (redish: -15 ℃<AirT≤ -5 ℃, blueish: AirT≤ -25 ℃) for early (Nov.-Dec.; ND) and late (Jan.-Feb.; JF) winter.

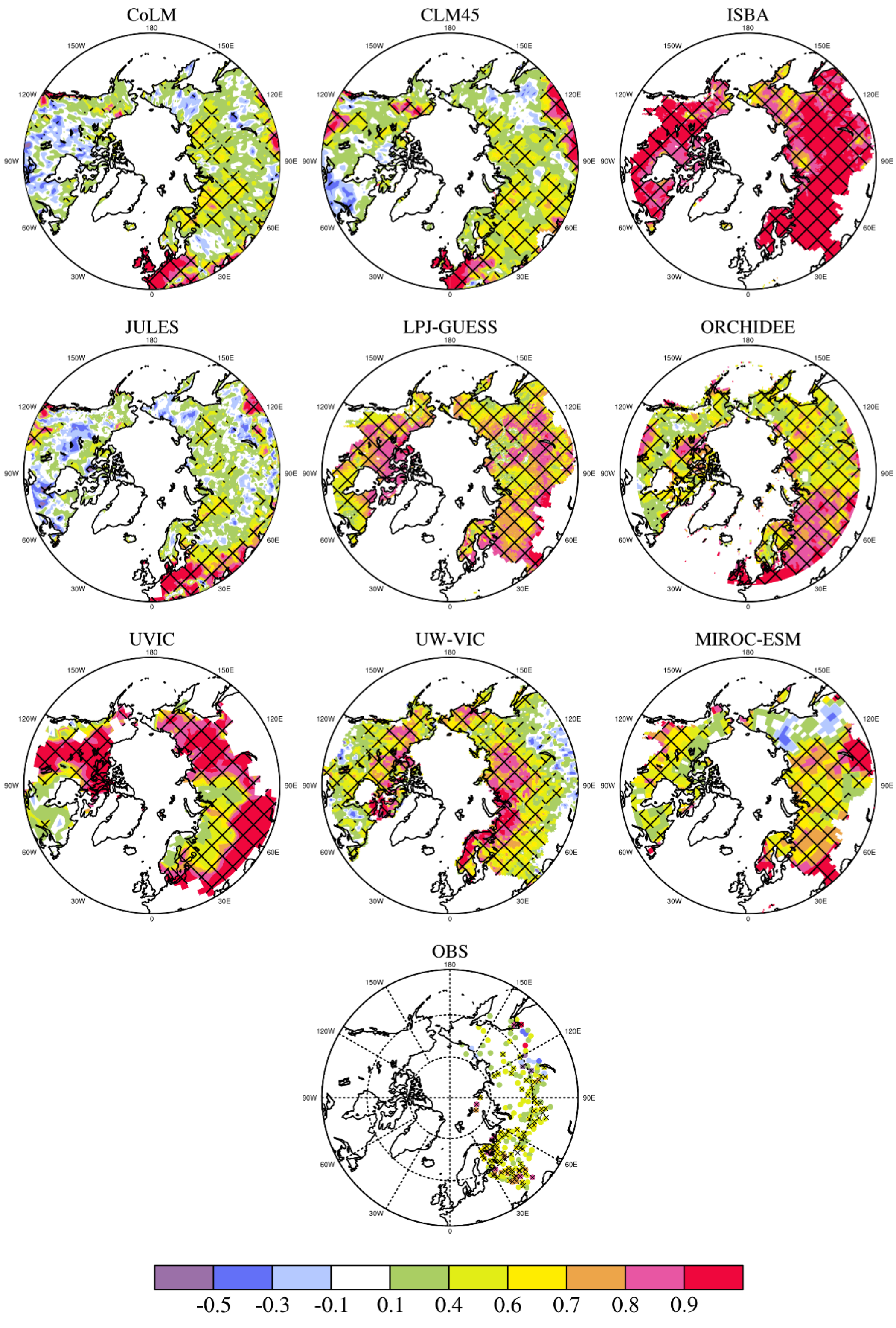

SI Figure 3. Spatial maps of the correlation coefficients between soil temperature at 20 cm depth and air temperature for winter 1980-2000. Regions with greater than 95% significance are hashed.

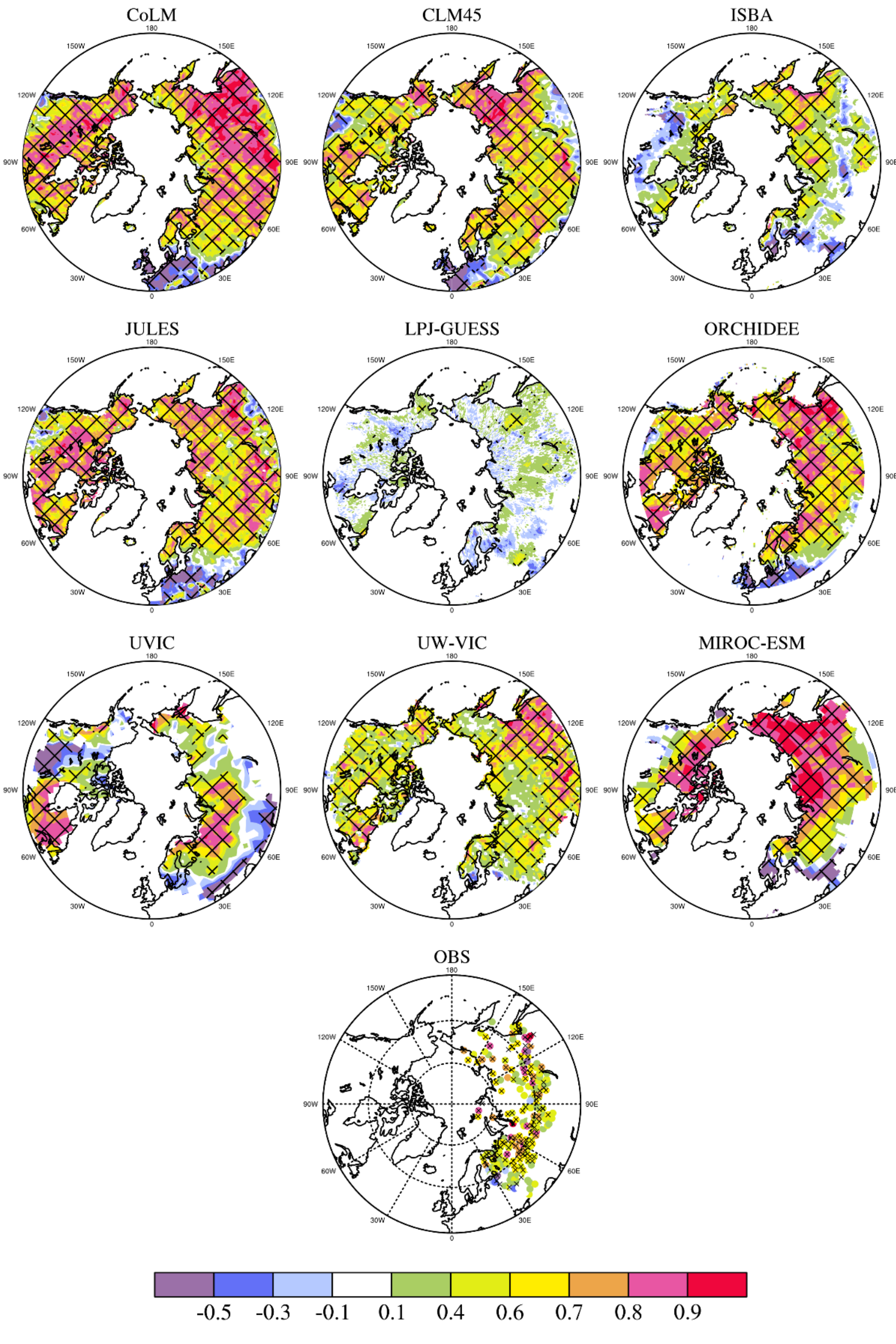

SI Figure 4. Spatial maps of the correlation coefficients between soil temperature at 20 cm depth and snow depth for winter 1980-2000. Regions with greater than 95% significance are hashed.

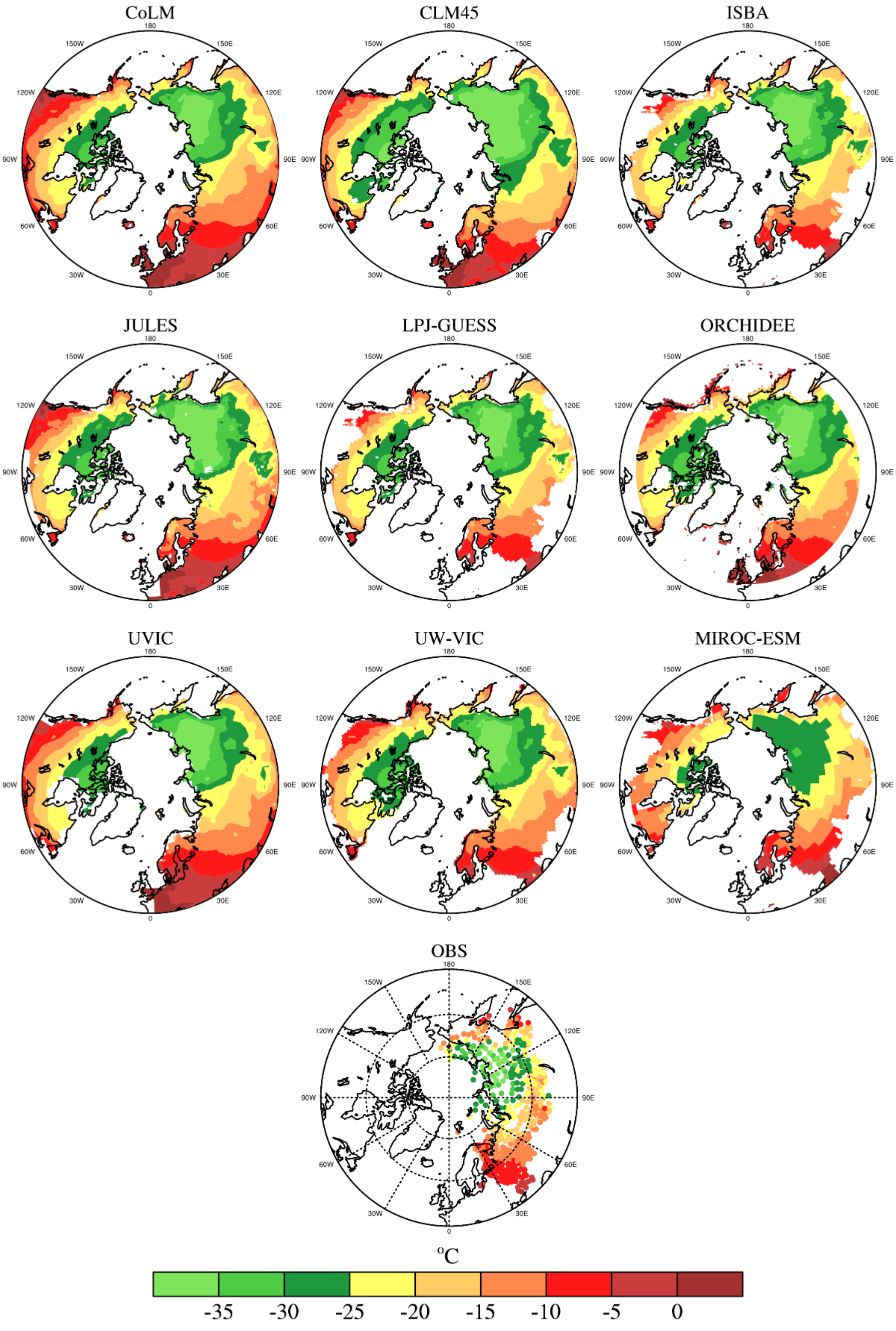

SI Figure 5. Spatial maps of mean air temperature (℃) for winter 1980-2000.

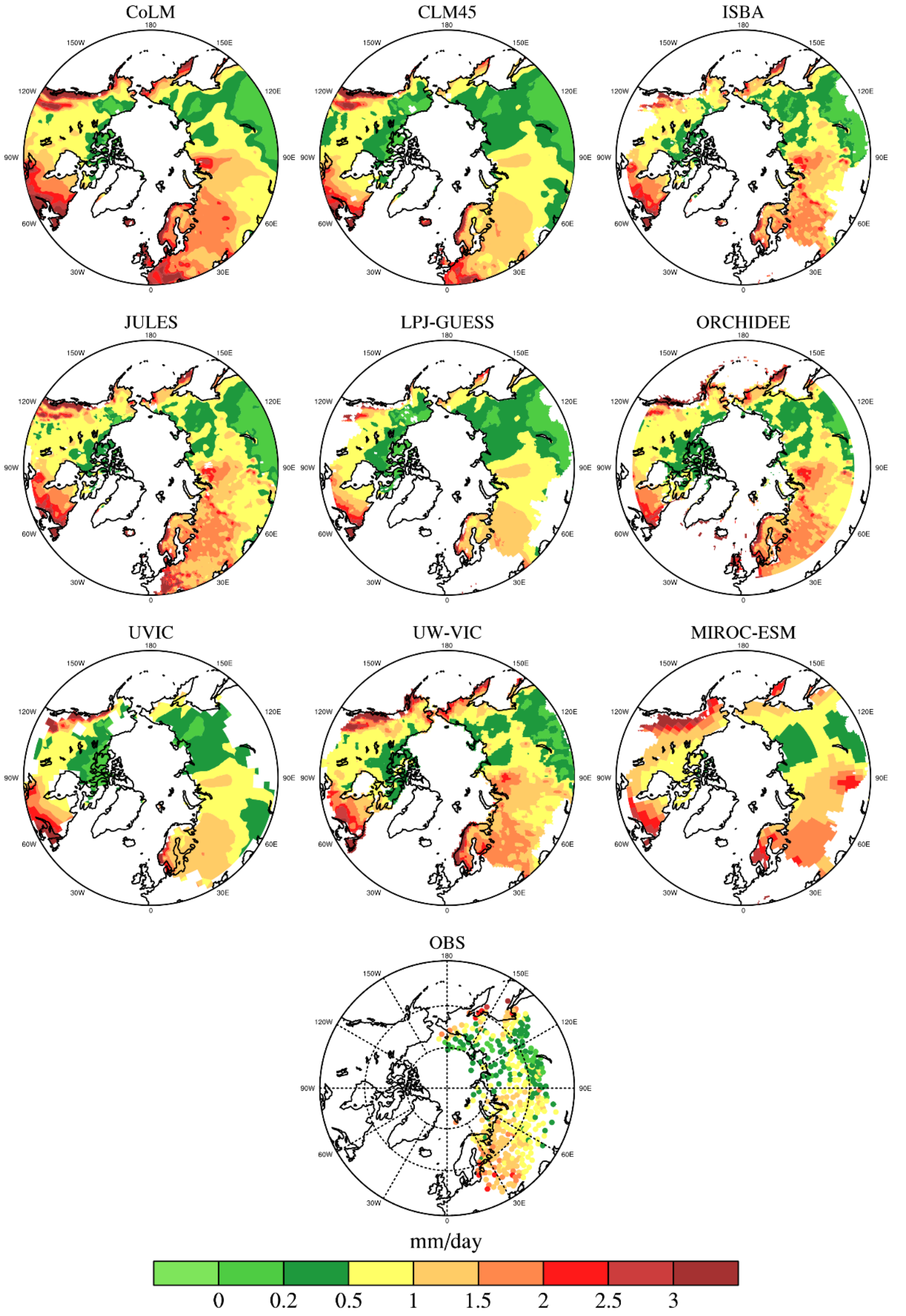

SI Figure 6. Spatial maps of mean precipitation (mm/d) for winter 1980-2000.

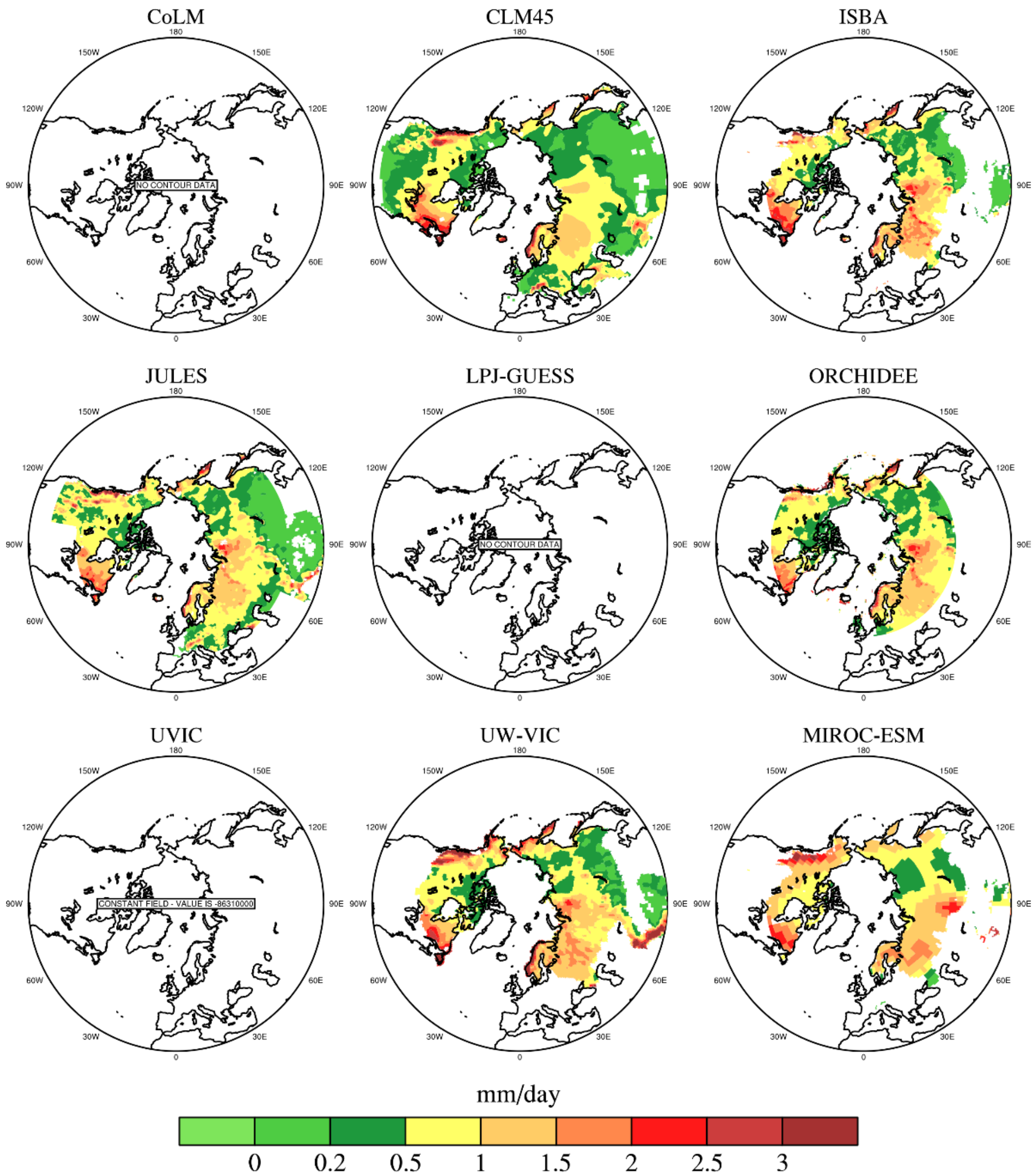

SI Figure 7. Spatial maps of snow fall (mm/d) for winter 1980-2000.

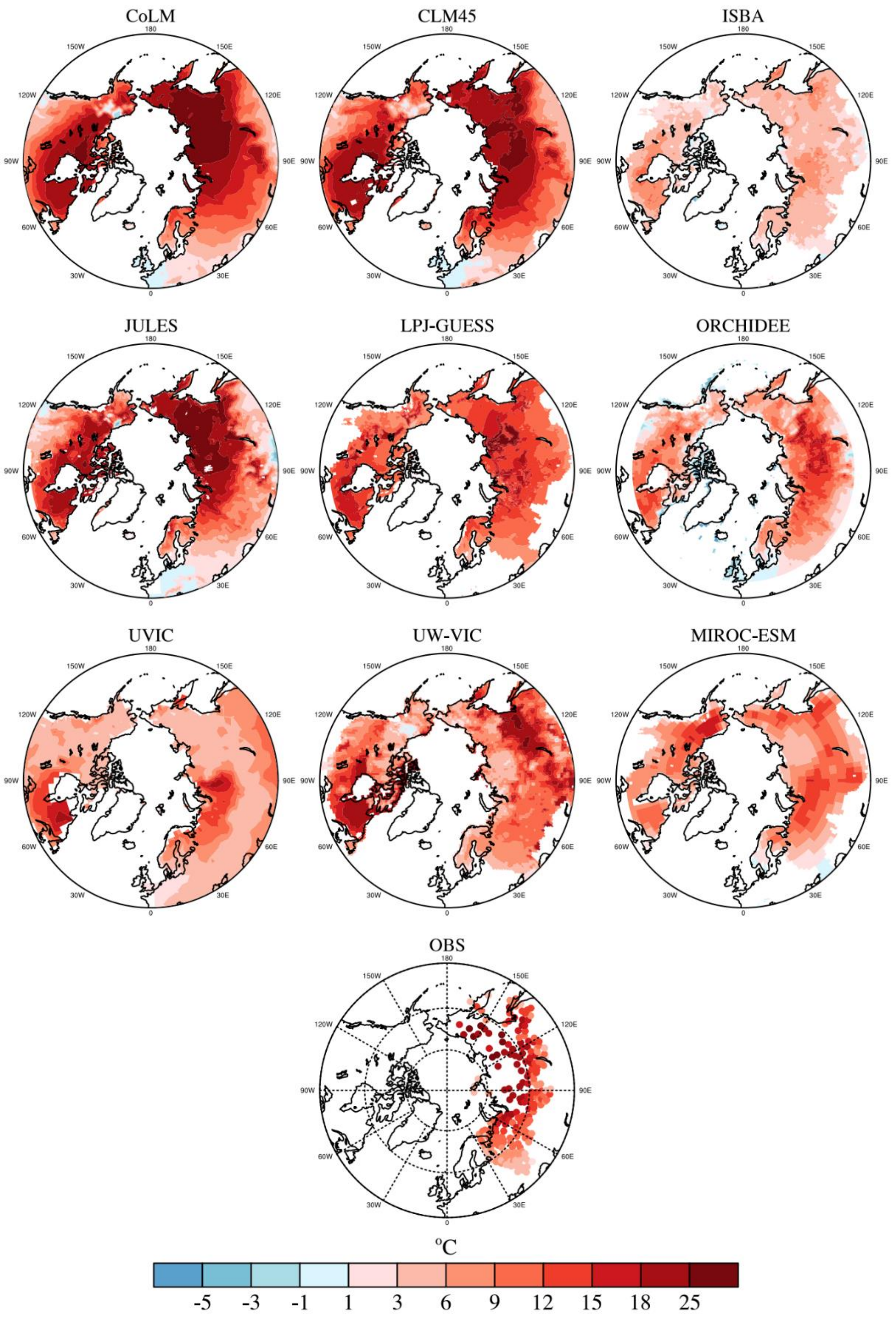

SI Figure 8. Spatial maps of ΔT (℃) (difference between soil temperature at 20 cm depth and air temperature) for winter 1980-2000.

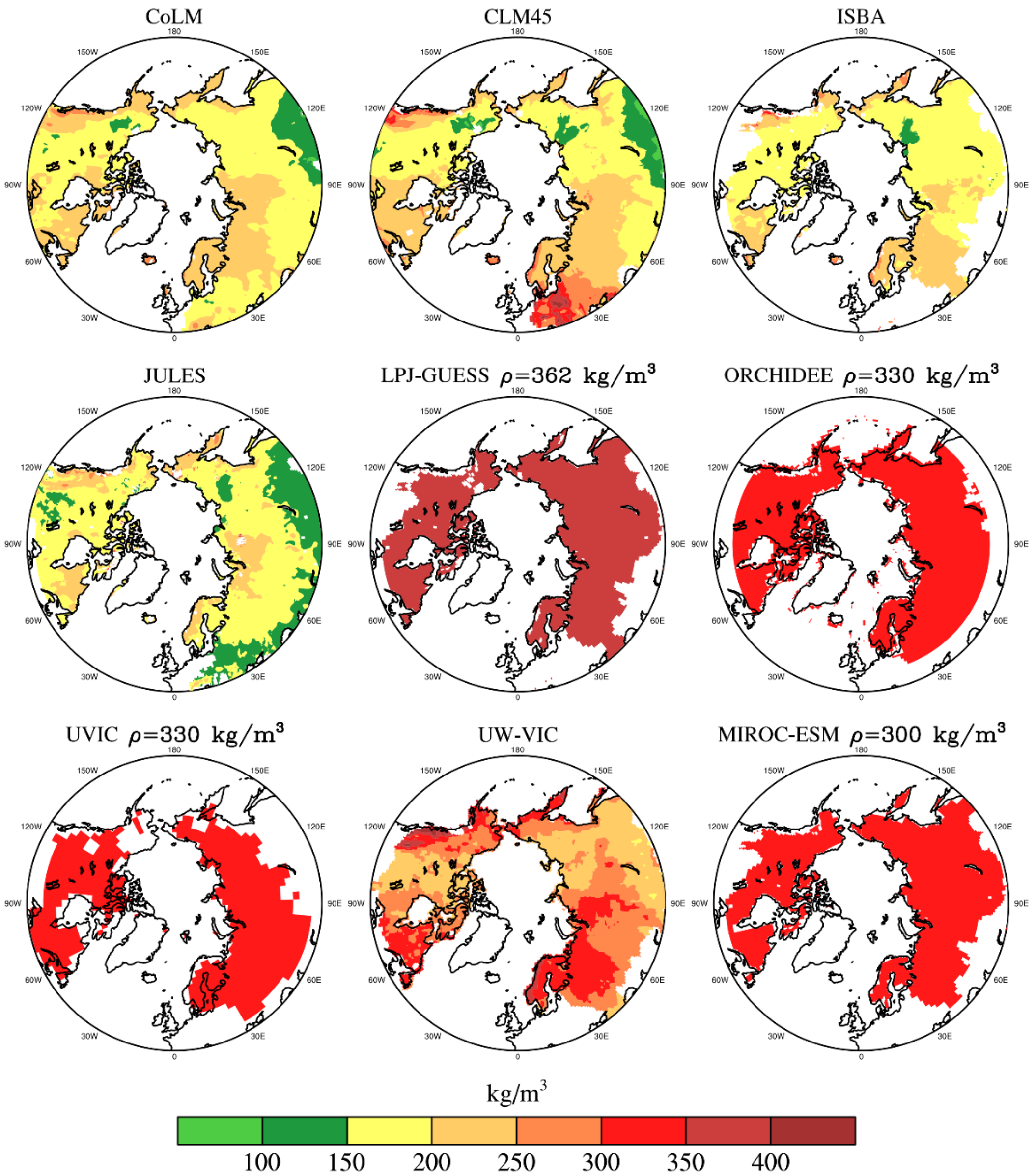

SI Figure 9. Spatial maps of snow density (kg m^{-3}) (calculated by the quotient of snow water equivalent and snow depth, if not directly output) for winter 1980-2000.